APPLE-II UNDULATOR MAGNETIC FIELDS CHARACTERISED FROM UNDULATOR RADIATION

K.P. Wootton*, R.P. Rassool, School of Physics, University of Melbourne, VIC, Australia
M.J. Boland, B.C.C. Cowie, Australian Synchrotron, Clayton, VIC, Australia

Abstract

The spatial profile of APPLE-II undulator radiation has been measured at high undulator deflection parameter, high harmonic and very small emittance. Undulators are typically designed to operate with small deflection parameter to push the fundamental mode to high photon energies. This unusual choice of parameters is desirable for measurement of vertical emittance with a vertical undulator.

We present 1-D and 2-D measured profiles of undulator radiation and show that this is reproduced in numerical models using the measured magnetic field of the insertion device. Importantly these measurements confirm that for these parameters, the spatial intensity distribution departs significantly from usual Gaussian approximations, instead resembling a double-slit diffraction pattern. This could be an important consideration for photon beamlines of ultimate storage ring light sources.

INTRODUCTION

Crucial to the vertical undulator emittance measurement technique we have developed is the availability of a high deflection parameter vertical undulator [1, 2]. At the Australian Synchrotron, we use an APPLE-II elliptically polarising undulator in a magnet phase configuration for vertically polarised light [3, 4]. The parameters of these experiments are summarised in Table 1.

Table 1: Undulator and Electron Beam Parameters for Experiment and Simulation

Parameter	Value
Electron beam energy	3.033 GeV
Beam energy spread	0.0011
Horizontal emittance	10 nm rad
Vertical emittance (nominal)	100 pm rad
Undulator K	3.85
Undulator period length	75 mm
Number of full periods	25
First harmonic photon energy	134.7 eV

UNDULATOR MAGNETIC FIELD

The model used in our previous analyses of the emittance measurements assumed an ideal horizontal, sinusoidal electron beam trajectory though the undulator. An improved model is presented which accounts for the deleterious effects of phase errors on the electron beam trajectory, using the measured magnetic field of the insertion device. The magnetic field profile of this APPLE-II insertion device was measured at the time of acceptance, at the design magnetic gap of 16.0 mm [4]. The magnetic field was measured along the device centreline with a three-axis Hall probe. Lamentably, at the time of writing we possess no equipment at the Australian Synchrotron with which to measure insertion device magnetic fields ourselves. For the purposes of safe clearance of the electron

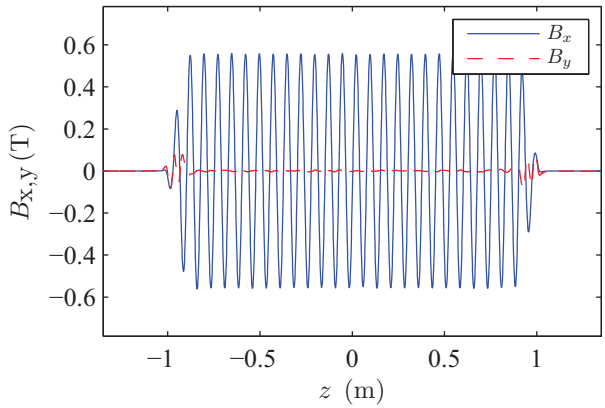

Figure 1: Magnetic field of APPLE-II insertion device in vertical polarisation mode, scaled from Hall probe measurements [4].

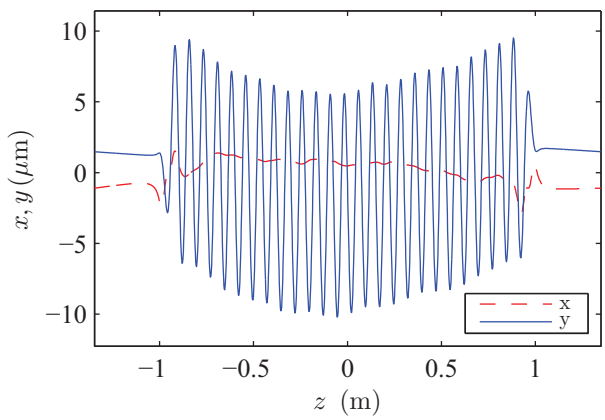

Figure 2: Trajectory of a 3 GeV electron beam through measured magnetic field map of Fig. 1 [4], calculated using SPECTRA [5].

* k.wootton@student.unimelb.edu.au

ISBN 978-3-95450-127-4

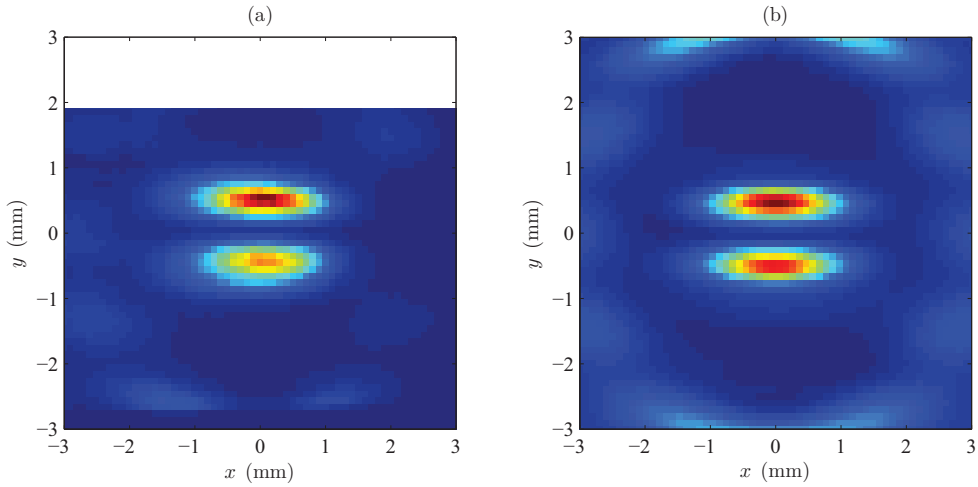

Figure 3: Spatial profile of undulator radiation from a vertical undulator, 15 m downstream of the insertion device. (a) Measured spatial profile of 6^{th} undulator harmonic, at 808 eV. (b) SPECTRA [5] simulation of spatial profile of 6^{th} undulator harmonic, at 808 eV. The magnetic field profile of Fig. 1 was used for the simulation of the insertion device.

beam vacuum chamber, we limit the minimum operating gap to 17.0 mm, and these experiments are conducted with a gap of 17.1 mm. To compensate for this in our model, the magnitude of the measured magnetic field components at a gap of 16.0 mm have been scaled down. The field was scaled down until the simulated on-axis peaks of the undulator harmonics were at the same photon energies as the measured spectrum. This scaled field is presented for the horizontal B_{x} and B_{y} components in Fig. 1.

The synchrotron radiation code SPECTRA was used to simulate light produced by the insertion device [5]. Using the field illustrated in Fig. 1, the trajectory of a 3 GeV electron was calculated and is shown in Fig. 2.

PINHOLE SCANS (2-D)

The angular distribution of spontaneous radiation from an undulator is theoretically described [6–8]. Devices of interest to storage ring lightsources typically employ undulators of small deflection parameter ($K \approx 1$), and prefer to use low undulator harmonics to achieve high photon beam brilliance. Figure 3 presents measurements and simulations of the projection of undulator radiation from this APPLE-II undulator.

The beamline used for these experiments does not have a pinhole for characterising the spatial profile of radiation [9]. Several other beamlines do, for this specific purpose [10]. Instead, we close four blades of the white-beam slits to form a rectangular pinhole aperture, which are scanned to measure the profile of Fig. 3. A photodiode which captures the full beam passed by the white-beam slits was used for this measurement.

The important features of Fig. 3 are the central two lobes of the 6^{th} harmonic, and the outer ring of the 7^{th} harmonic. This narrow interference pattern is characteristic of undulator radiation, but is seldom observed. Storage ring light sources typically operate with very large horizontal emittances of order nm rad, convolving the narrow angular distribution of undulator radiation with the broad horizontal beam emittance. The interference pattern is observed here specifically because of the vertical deflection by the undulator and the low vertical emittance of order pm rad.

Integrating over the central 3 mm width of the distribution in Fig. 3, the vertical profile of undulator radiation at 808 eV is presented in Fig. 4.

Figure 4 highlights that the measured vertical asymmetry in the distribution of undulator radiation is partially accounted for by using the measured magnetic field distribution in simulations. The central on-axis null at $y = 0$ mm is similarly well-described.

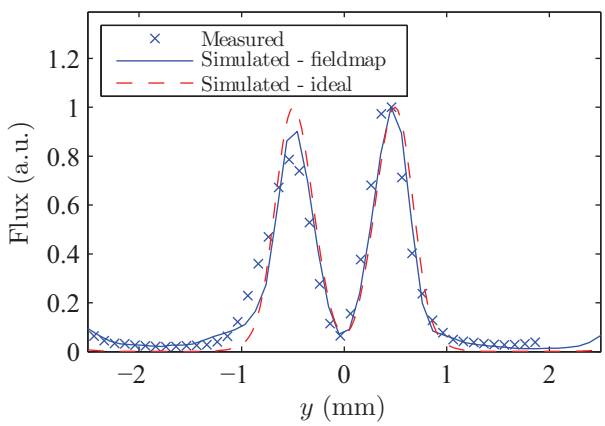

Figure 4: Vertical profile of undulator radiation in Fig. 3. The intensity is integrated over $x = -1.5$ mm to 1.5 mm.

ISBN 978-3-95450-127-4

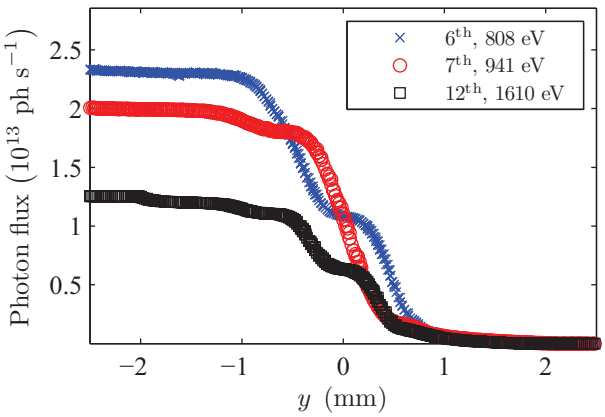

Figure 5: Measured undulator radiation intensity blade scans at different undulator harmonics. The lower white-beam slit is scanned vertically upwards from $y < 0$ to $y > 0$.

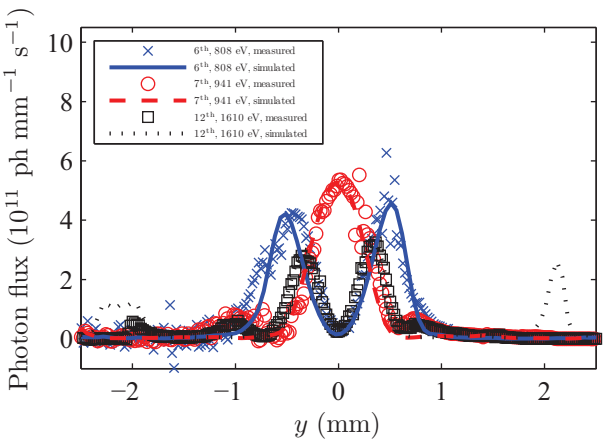

Figure 6: Gradient of Fig. 5 with respect to vertical blade scan direction. The vertical profile of undulator radiation is recovered and is compared to simulation. Compare also with Fig. 4.

BLADE SCANS (1-D)

The spatial profile of radiation was characterised in the vertical direction alone using blade scans. With a horizontal aperture of 0.5 mm, the lower blade of the white beam slits was stepped vertically upwards through the radiation distribution. The change in measured photon flux through the aperture with blade position is plotted in Fig. 5. Taking the derivative of this distribution with respect to the vertical position of the blade, the intensity distribution of undulator radiation is recovered. This is plotted in Fig. 6.

DISCUSSION

These measurements confirm assumptions regarding the spatial distribution of undulator radiation, which is sensitive to vertical emittance. The angular distribution of undulator radiation departs from usual Gaussian approximations, and at such low emittances resembles a narrow interference diffraction pattern. This is observed because the vertical emittance is so small relative to the transverse deflection of the undulator in the vertical direction.

Low emittance light sources are beginning to produce undulator radiation of interesting spatial distributions [10]. As electron beam light sources approach diffraction limits, the spatial distribution of radiation may become a topic of interest. Diffraction-limited ultimate storage rings are currently proposed with horizontal emittance of order 100 pm rad [11–13]. Such proposals should be aware of the diffraction-limited spatial distribution of undulator radiation, and its departure from usual Gaussian-approximated, emittance dominated photon beams.

CONCLUSION

The spatial distribution of radiation from a vertical insertion device has been characterised at very low vertical emittance. Both 2-D and 1-D spatial distributions of radiation have been measured, using a combination of blade scans. Simulations of the insertion device radiation are given, using a magnetic field distribution scaled from the measured field. It is shown that these simulations accurately reproduce the measured photon beam distribution. This close agreement between simulation and experiment is important both for the vertical emittance undulator technique, and potentially also for insertion devices at proposed ultimate storage ring light sources.

ACKNOWLEDGEMENTS

KPW is very grateful for useful discussions with Takashi Tanaka (SPring-8) in the implementation of measured magnetic field distributions within the SPECTRA code. This research was undertaken on the soft x-ray beamline on the storage ring at the Australian Synchrotron, Victoria, Australia.

REFERENCES

[1] K.P. Wootton, et al., Phys. Rev. Lett. **109** (19), 194801 (2012).

[2] K.P. Wootton, et al., Proceedings of IBIC 2012, Tsukuba, Japan, MOCB04 (2012).

[3] S. Sasaki, Nucl. Instrum. Methods A **347**, 83 (1994).

[4] C. Ostenfeld, et al., Proceedings of PAC 2007, Albuquerque, USA, TUPMN006, June (2007).

[5] T. Tanaka and H. Kitamura, J. Synch. Rad. **8**, 1221 (2001).

[6] H. Motz, J. Appl. Phys. **22**, 527 (1951).

[7] K.-J. Kim, Nucl. Instrum. Methods A, **246** 67 (1986).

[8] H. Wiedemann, Particle Accelerator Physics, 3rd ed., Springer-Verlag, Berlin, Germany (2007).

[9] B. C. Cowie, A. Tadich, and L. Thomsen, AIP Conf. Proc. **1234**, 307 (2010).

[10] J. Bahrdt, et al., Phys. Rev. Lett., **111**, 034801 (2013).

ISBN 978-3-95450-127-4

[11] M. Bei, et al., Nucl. Instrum. Methods A **622**, 518 (2010).

[12] Y. Shimosaki, et al. Proceedings of IPAC 2012, New Orleans, USA, TUPPC014, May (2012).

[13] L. Farvacque, et al. Proceedings of IPAC 2013, Shanghai, China, MOPEA008, May (2013).

ISBN 978-3-95450-127-4